

Performance of the low pressure MWPCs for fission fragments under a high background*

SONG Yu-Shou(宋玉收)^{1,1)} Margaryan A.² HU Bi-Tao(胡碧涛)³ TANG Li-Guang(唐力光)^{4,5}

¹ College of Nuclear Science and Technology, Harbin Engineering University, Harbin 150001, China

² Yerevan Physics Institute, Yerevan 375036, Armenia

³ School of Nuclear Physics and Technology, Lanzhou University, Lanzhou 730000, China

⁴ Thomas Jefferson National Accel. Facility, Newport News, VA 23606, USA

⁵ Department of Physics, Hampton University, Hampton, VA 23668, USA

Abstract: Two couples of low pressure multi-wire proportional chambers (MWPC) were located in the target chamber to detect fission fragments in a hypernuclei producing experiment at Thomas Jefferson National Laboratory (Jlab). In the experiment, a continuous wave (CW) electron beam was applied to form hypernuclei by electromagnetic interaction. In the target chamber, the high energy (1.853 GeV) and high intensity (500 nA) primary electron beam caused a high particle background, which influenced the detection of the fission fragments. This report described the design of the MWPCs and studied the fission-fragment detecting performance of them under such a high background. The efficiency of the MWPCs was given with the help of a high resolution kaon spectrometer. At the same time, the background particles were discussed with a Monte Carlo code based on GEANT4.

Key words: MWPC, fission fragment, background, detecting performance

PACS: 29.30.Aj **DOI:** 10.1088/1674-1137/35/8/011

1 Introduction

A low-pressure MWPC (LPMWPC) is widely used as a beam monitoring detector in front of a target for its high counting rate capability and negligible disturbance for the beam [1, 2]. At the same time, one can use it to detect some special particles or ions by tuning the working gas pressure [3, 4]. The Jlab experiment E02-017 had been proposed to explore the way to measure the lifetime of heavy hypernuclei of ${}_{\Lambda}^{209}\text{Pb}$ directly and the reaction ${}^{209}\text{Bi}(e, e'K^+)_{\Lambda}^{209}\text{Pb}$ and ${}^{209}\text{Bi}(\gamma, K^+)_{\Lambda}^{209}\text{Pb}$ was utilized to produce the hypernuclei. Among the nuclei medium, a Λ will dominantly decay by a non-mesonic way $N + \Lambda \rightarrow N + N + 176 \text{ MeV}$ [5, 6]. The released energy is high enough to cause the fission of a hypernucleus. This makes it possible to measure the lifetime of heavy hypernuclei directly. Two cou-

ples of LPMWPC with gas pressure around 200 Pa forming a two-arm fission fragments detector (FFD) were used to detect the fission fragments(FF). The FFD has nearly 100% of fission fragments detecting efficiency [4] and high time resolution of ~ 163 ps [7] during the test by a ${}^{252}\text{Cf}$ spontaneous source. The high luminosity electron beam created high background particles when it arrived at the target chamber, which crashed the time resolution and the detecting efficiency of the FFD. By the coincidence between FFD and a high kaon spectrometer (HKS) [8] which was used to detect kaons produced in the reaction ${}^{209}\text{Bi}(e, e'K^+)_{\Lambda}^{209}\text{Pb}$, the fission fragments detecting efficiency were given under the experimental condition. The effect of the background particles on the FF detection were also analysed by a Monte Carlo simulation. The LPMWPC technique and the CW electron beam of Jlab shed light on the direct measurement of the lifetime of heavy hypernuclei.

Received 12 October 2010

* Supported by Fundamental Research Funds for Central Universities (HEUCF101501), Fundamental Research Funds of Harbin Engineering University (002150260713) and National Natural Science Foundation of China (10575046)

1) E-mail: songyushou.cn@yahoo.com.cn

©2011 Chinese Physical Society and the Institute of High Energy Physics of the Chinese Academy of Sciences and the Institute of Modern Physics of the Chinese Academy of Sciences and IOP Publishing Ltd

2 Experimental setup

This experiment was performed by using part of the setup of the Jlab experiment E01-011 in Hall C [5]. It (Fig. 1) consists of two major parts: magnetic spectrometer HKS with front splitter magnet and FFD located in the target chamber. The scattered electrons were not tagged in this experiment. The electron beam pipe was terminated before the E01-011 splitter magnet and the FFD was inserted in the gap between the beam exit window and the entrance vacuum window of the splitter magnet. The target for this experiment was mounted in the cen-

ter of the FFD. The incidence electrons had to pass through the stainless steel foil vacuum window for the terminated beam pipe, ~ 20 cm air and $250 \mu\text{m}$ thick Al window for FFD with a 5% radio length Cu foil mounted on it. Therefore, intensive real photons with wide energy range were produced from these materials and incident to the tilted thin Bi target foil together with the beam electrons. The primary beam electrons, scattered electrons and forward produced particles, i.e. protons, pions and positrons, exited the FFD through a $250 \mu\text{m}$ Al window. The positive particles from the primary reaction were detected by the following HKS and the associated fission fragments by FFD.

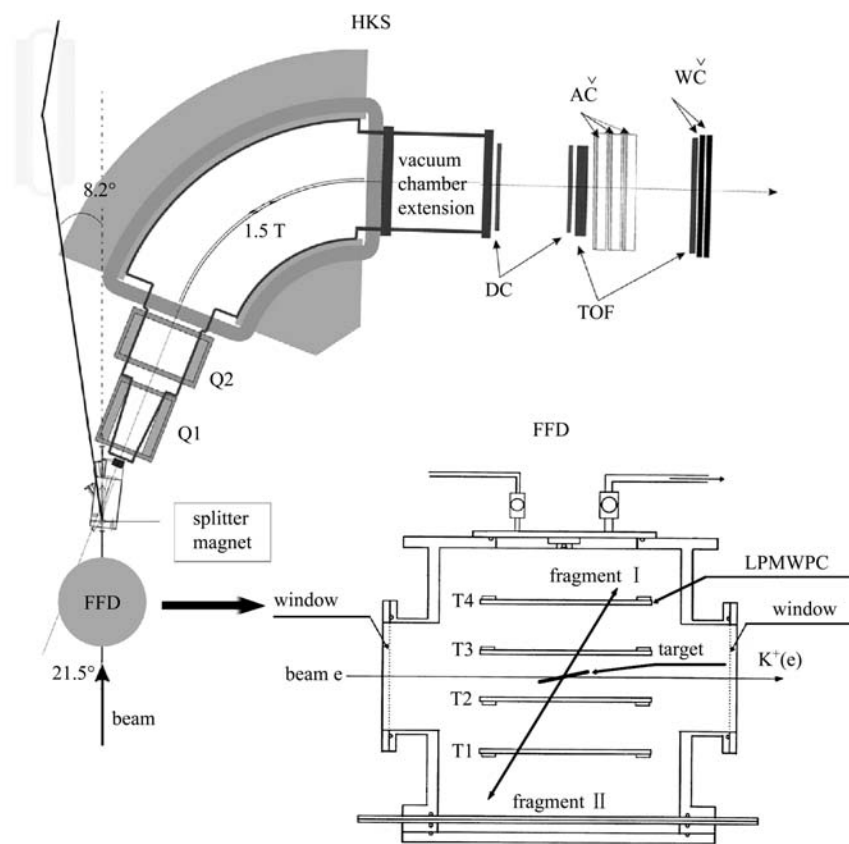


Fig. 1. Schematic view of the experimental setup.

3 Design and operation of the FFD

The FFD consists of four windowless LPMWPC chamber units, which form two symmetric arms placed on the sides (top and bottom) of the central beam. The four LPMWPCs are tagged as T1, T2, T3, T4 from bottom to top. The outer chambers (T1, T4) and the inner chambers (T2, T3) have different active areas— $149 \text{ mm} \times 149 \text{ mm}$ and $209 \text{ cm} \times 209 \text{ cm}$. Each

arm provides ~ 1.8 sr of solid angle coverage. During the experiment, the FFD is placed in the vacuum target chamber, which is connected to a vacuum pumping system and can be evacuated to a pressure ~ 0.1 Pa. It is also equipped with stainless-steel valves for gas handling and two barometers for pressure measurement. The chamber volume is connected to a reservoir of liquid heptane (C_7H_{16}), with a reducing valve and filled with 200–300 Pa of gas vapor.

The target is located at the center of the two detecting arms and is made of a thin foil of ^{209}Bi with a thickness of 2 mg/cm^2 . It is placed at a small tilt angle of about 10 degrees with respect to the beam direction so that the effective target thickness is about 14 mg/cm^2 . Such target orientation is also used to minimize the target thickness so that FF can exit the target towards the LPMWPCs with a maximized production rate.

Each LPMWPC unit of the FFD has the same structure as shown in Fig. 2(a) consisting of five electrodes made of wire planes [4]. The frames of the electrodes are made of G10 (a kind of glass textolite) with a thickness of 3 mm, which is also the plane spacing. The central electrode is a wire-anode plane from which the time signal is extracted. Due to the large active area of the LPMWPC, a passive mean timing is made in grouping the anode wires to minimize the position dependence of the time resolution as shown in Fig. 2(b). The anode is placed between two cathode wire planes which have their wires oriented at an angle of 90° with respect to each other. Both the anode and cathode planes have wire spacing of 1 mm. The anode plane used $20\text{ }\mu\text{m}$ diameter gold-plated tungsten wire, while the cathode plane used $40\text{ }\mu\text{m}$ diameter copper-beryllium wires. By a

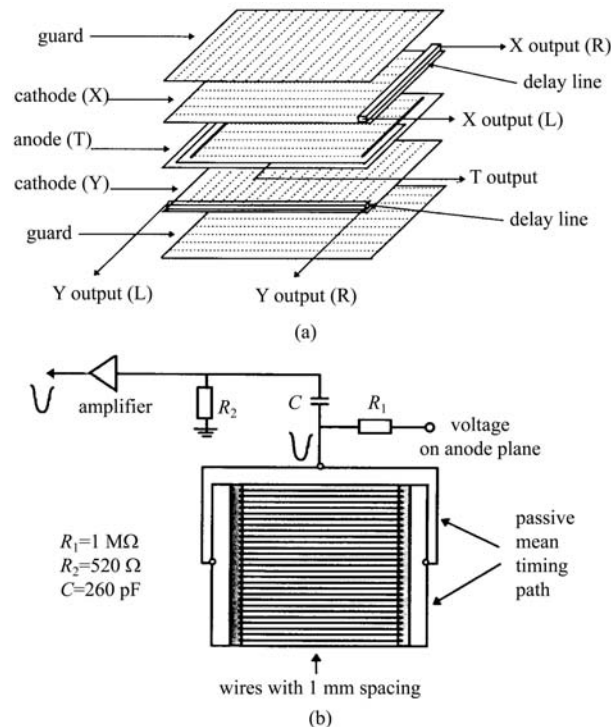


Fig. 2. (a) The schematic structure of a single LPMWPC unit, where the dashed line means the wire direction. (b) The configuration of the anode wire plane of a single LPMWPC unit.

time division method, the cathode is designed to give the position information, which was not used in this experiment.

The cathode wires are at a potential of -100 V . Additionally, the grounded guard electrodes outside the cathode planes are used to avoid the charges deposited outside the LPMWPC. The usual potential applied to the anode is about $+400\text{ V}$. When applying $+370\text{ V}$ to the anode plane, -100 V on the cathodes and 0 V on the guard planes, we have about 100 mV signals. The typical time resolution is 150 ps tested by ^{252}Cf spontaneous source. The LPMWPC can also be operated in a double step regime. In this case, we apply negative voltage to the guard plane and positive voltage to the anode plane and have the cathode plane at ground.

During the test, the FFD worked well with all the experimental instruments powered down. However we found out that the HKS spectrometer magnet power supply system induces radioactive frequency (RF) noise into the FFD. The RF noise induced directly to the wire planes of LPMWPCs passes the same way as the electrical signals from FF. Therefore, it was impossible to avoid the induced noise by proper grounding of the experimental setup. In addition the noise has the similar structure and amplitude as real signals from FFD operated in a single step regime and appears with about a 50% duty factor, which means that the expected trigger rates would be determined mainly by the induced RF noise. We tried to avoid the noise problem by operating the FFD in a double step regime. In this case the amplitude of real signals was several times larger than the noise level, so it was possible to eliminate the induced noise by proper selection of the timing discriminator levels. Applying -250 V to the guard plane and $+250\text{ V}$ to the anode, we had 500 mV signals by the same test and the corresponding time resolution is about 200 ps .

4 Experimental results and discussion

Additional problems arose when the electron beam was given. Passing through the target chamber window and the bismuth target the intensive incident electron beam of 500 nA , i.e. $\sim 3 \times 10^{12}\text{ e/s}$, produced a huge amount of background particles. To consider the background particles a Monte Carlo simulation based on GEANT4 [9] was performed. Fig. 3 gives the intensity I_{bk} of the background particles of an outer LPMWPC and an inner one. The background is dominantly composed of electrons—mainly

δ -electrons except very few scattered primary electrons crossing through the LPMWPCs. These electrons do not make the LPMWPCs firing, but they will increase the dark current level and operational conditions of the FFD, when they pile up around an anode [10, 11]. Due to such background particles, the amplitude of signals from LPMWPCs, especially from the planes close to the target are essentially decreased. At the same time, it was impossible to increase the signal amplitude by increasing the operational voltages of LPMWPCs, because the inner LPMWPC units started sparking when working with the anode voltages of +340 V, which was 60 V lower than that of the case without a beam. It was also impossible to operate the FFD in a double step regime. With the beam we were able to operate the FFD in a single step mode only, applying -130 V, $+300$ V and 0 V to cathode, anode and guard planes.

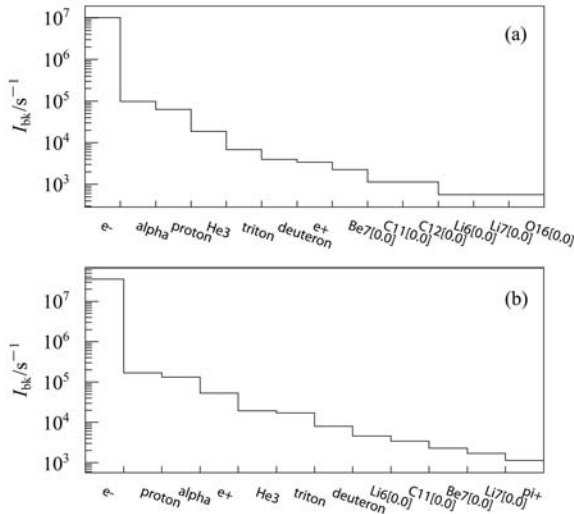


Fig. 3. A Monte Carlo simulation code based on GEANT4 gives the intensity I_{bk} of different background particles across (a) an outer LPMWPC and (b) an inner LPMWPCs respectively, when the beam intensity is 500 nA.

The intensity of δ electrons across an inner LPMWPC $I_{ebki} \approx 3.0 \times 10^7$ e/s, is about 3 times the background δ -electron intensity ($I_{ebko} \approx 1.0 \times 10^7$ e/s) across an outer LPMWPC. To study the influence of the background on the timing signals output from an LPMWPC anode, we changed the background condition by reducing the primary incidence electron beam intensity I_e from 500 nA to 100 nA. The typical timings from four LPMWPC anode planes, T1, T2, T3 and T4 are shown in Fig. 4. The I_{ebki} with $I_e=100$ nA should be smaller than I_{ebko} with $I_e=500$ nA. However, there is no clue that the timing signals from inner LPMWPCs with $I_e=100$ nA are better than

those from the outer LPMWPC with $I_e=500$ nA. The study on the background density (intensity per unit area) gives the answer. The background particles concentrate around the symmetry axis of the inner LPMWPC planes along the electron beam direction where the corresponding background density is higher. If the fission fragments fly through such background concentrated area, the corresponding signal amplitudes will be decreased dramatically. Since the performance of the inner LPMWPCs was not satisfying even by reducing the intensity of the incidence electron beam, the experiment had been run with $I_e=500$ nA, which could provide more hyperon production within a limited experiment interval.

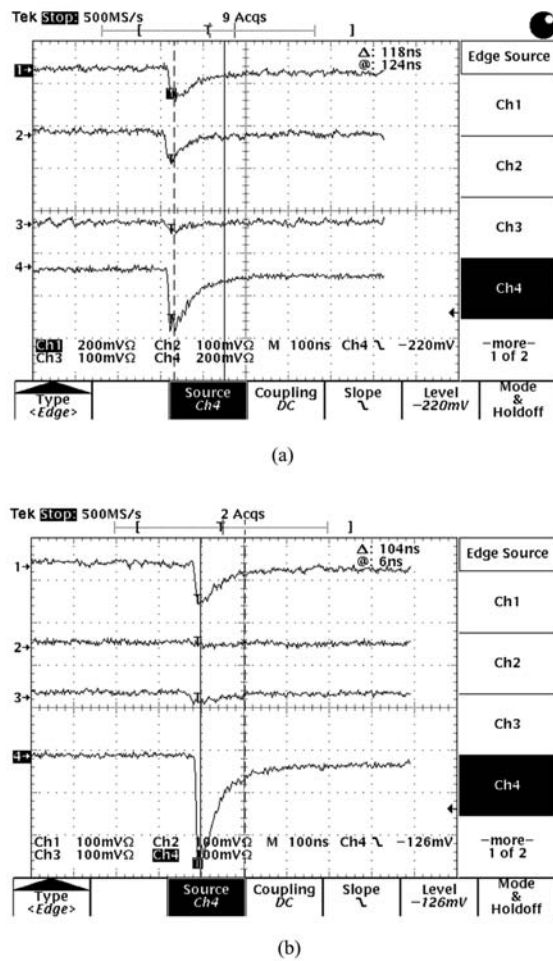


Fig. 4. The output signals from FFD modules with (a) electron beam intensity of $I_e=100$ nA (b) and electron beam intensity of $I_e=500$ nA. The signals of Channel 1, Channel 2, Channel 3, Channel 4 correspond to those from T1, T2, T3, T4.

Besides the δ -electrons there are lots of other light charged ions like protons, α particles, which could be

detected by the FFD with some low efficiency. However, this would not influence the experimental result because such events could be eliminated by the coincidence with the kaons identified by HKS [8].

When Λ -hypernuclei are produced, they may be highly excited and fission (prompt fission) before any de-excitation; the survival hypernuclei, which de-excite by emitting photons and nucleons, are stable with respect to electromagnetic and strong processes. They decay by the nonmesonic weak interaction and cause delayed fissions. In this experiment, both prompt fissions and delayed fissions can be detected by the FFD. Once a kaon is detected by HKS, it means a Λ comes into being. By some rate R_{Kf} the fission happens and fission fragments fly uniformly in 4π directions. Thus, the number of detected fissions associated with kaons on each plane can be expressed as

$$n_i = N_K R_{Kf} \Omega_i \varepsilon_i \quad (i = 1, 2, 3, 4), \quad (1)$$

where N_K is the number of kaons identified by HKS, R_{Kf} is the fission rate per kaon, Ω_i is the acceptance rate of the LPMWPCs and ε_i is the fission fragments detecting efficiency of the LPMWPCs. By the coincidence of HKS·TDC1 $n_1 = 440 \pm 55$ was given; by the coincidence of HKS·TDC4 $n_4 = 494 \pm 51$ was given; and by the coincidence of HKS·TDC1·TDC4 we obtained $n_{14} = 111 \pm 28$ (without special description the given errors are statistical ones). The identified kaon number is 61780 [8]. Due to the symmetrical geometrical configuration of the LPMWPC planes, the solid acceptance rates satisfy $\Omega_{out} = \Omega_1 = \Omega_4$ and $\Omega_{in} = \Omega_2 = \Omega_3$, where $\Omega_{out} \approx 15\%$ and $\Omega_{in} \approx 31\%$ are the acceptance rates of outer planes and inner planes

of the FFD. Since the fission can be looked as back to back due to momentum conservation, if a fragment is detected by one arm the other fragment will aim automatically within the solid angle acceptance of the other arm on the opposite side. Therefore, the events number n_{14} of coincidence between kaons and back to back fissions is written as

$$n_{14} = N_K R_{Kf} \Omega_{out} \varepsilon_1 \varepsilon_4. \quad (2)$$

Based on Eq. (1) and Eq. (2) we can obtain the efficiency of planes $\varepsilon_1 = (23 \pm 7)\%$ and $\varepsilon_4 = (25 \pm 8)\%$. In a similar way, we estimated that the efficiencies of T2 and T3 were below 5%.

5 Summary

For the first time, the LPMWPC technique was used for FF detection in a hyperon production experiment. By this experiment we studied the working conditions of the FFD made up of four LPMWPCs. The FF-detecting performance of an LPMWPC depends not only on the total background but also on the background spacial density. With the setting of the FFD and the incidence electron beam intensity in experiment, the inner LPMWPCs can hardly give an effective result. The effective methods to improve the experiment are to increase the distance between the detection units of the FFD and the beam axis or reduce the incidence beam intensity, which will extend the beam time to obtain the same magnitude of experimental data. At the same time, the RF noise is also a problem which needs to be conquered.

References

- 1 Korshennikov A A, Nikolskii E Yu, Bertulani C A et al. Nucl. Phys. A, 1997, **617**: 45
- 2 Neumaier S R, Alkhozov G D, Andronenko M N et al. Nucl. Phys. A, 2002, **712**: 247
- 3 Margarian A T. Nucl. Instrum. Methods A, 1995, **357**: 495
- 4 Assamagan K, Baker K, Bayatyan G et al. Nucl. Instrum. Methods A, 1999, **426**: 405
- 5 Hashimoto O, Tamura H. Prog. Part. and Nucl. Phys., 2006, **57**: 564
- 6 Hagino K, Parreño A. Phys. Rev. C, 2001, **63**: 044318
- 7 SONG Yu-Shou, LUO Wei, TANG Li-Guang et al. HEP & NP, 2007, **31**: 755 (in Chinese)
- 8 SONG Yu-Shou, HU Bi-Tao. Chinese Physics C, 2009, **33**: 423
- 9 Allison J, Amako K, Apostolakis J et al. IEEE Trans. Nucl. Sci., 2006, **53**: 270
- 10 Dematt L, Hamsch F J, Bax H et al. Nucl. Instrum. Methods A, 2002, **480**: 706
- 11 Crittenden R R, Ems S C, Heinz R M et al. Nucl. Instrum. Methods, 1981, **185**: 75